Supporting Information

Characterization of human UDP-glucuronosyltransferases responsible for glucuronidation and inhibition of norbakuchinic acid, a primary metabolite of hepatotoxicity and nephrotoxicity component bakuchoil in *Psoralea corylifolia* L.

Zhihong Yao,†*[ab] Shishi Li,†[a] Zifei Qin,*[abc] Xiaodan Hong,[ad] Yi Dai,[ab] Baojian Wu,[ab] Wencai Ye,[abc] Frank J Gonzalez[e] and Xinsheng Yao[abcd]

[a]College of Pharmacy, Jinan University, Guangzhou 510632, P.R. China;

[b]Guangdong Provincial Key Laboratory of Pharmacodynamic Constituents of TCM and New Drugs Research, College of Pharmacy, Jinan University, Guangzhou 510632, P.R. China;

[c]Integrated Chinese and Western Medicine Postdoctoral research station, Jinan University, Guangzhou 510632, P.R. China;

[d]Guangzhou Research and Creativity Biotechnology Co. Ltd, Guangzhou, 510663, P. R. China;

[e]Laboratory of Metabolism, Center for Cancer Research, National Cancer Institute, National Institutes of Health, Bethesda, Maryland 20892, USA;

†These two authors contributed equally to this work.

*Author to whom correspondence should be addressed.

E-mail: tyaozh@jnu.edu.cn; yaozhihong.jnu@gmail.com (Zhihong Yao);

E-mail: qzf1989@163.com (Zifei Qin);

Figure Caption

Figure S1 MS/MS spectra of norbakuchinic acid and its two glucuronides.

Figure S2 Kinectic profiles for glucuronidation of norbakuchinic acid by various types of microsomes. (a) monkey liver microsomes (MkLM); (b) rat liver microsomes (RLM); (c) guinea pig liver microsomes (GpLM); (d) rabbit liver microsomes (RaLM); (e) dog liver microsomes (DLM); (f) mice liver microsomes (MLM); In each panel, the insert figure showed the corresponding Eadie-Hofstee plot. All experiments were performed in triplicate.

Figure S3 Inhibition evaluation of NBKA toward Expressed UGT1A6-catalyzed 4-MU glucuronidation. Concentration-dependent plot (a) and Dixon plot (b) of NKBA's inhibition toward recombinant UGT1A6-catalyzed 4-MU glucuronidation. All experiments were performed in triplicate.

Figure S4 Inhibition evaluation of NBKA toward Expressed UGT1A7-catalyzed 4-MU glucuronidation. Concentration-dependent plot (a) and Dixon plot (b) of NKBA's inhibition toward recombinant UGT1A7-catalyzed 4-MU glucuronidation. All experiments were performed in triplicate.

Figure S5 Inhibition evaluation of NBKA toward Expressed UGT1A8-catalyzed 4-MU glucuronidation. Concentration-dependent plot (a) and Dixon plot (b) of NKBA's inhibition toward recombinant UGT1A8-catalyzed 4-MU glucuronidation. All experiments were performed in triplicate.

Figure S6 Inhibition evaluation of NBKA toward Expressed UGT1A9-catalyzed propofol glucuronidation. Concentration-dependent plot (a) and Dixon plot (b) of NKBA's inhibition toward recombinant UGT1A9-catalyzed propofol glucuronidation. All experiments were performed in triplicate.

Figure S7 Inhibition evaluation of NBKA toward Expressed UGT1A10-catalyzed 4-MU glucuronidation. Concentration-dependent plot (a) and Dixon plot (b) of NKBA's inhibition toward recombinant UGT1A10-catalyzed 4-MU glucuronidation. All experiments were performed in triplicate.

Figure S8 Inhibition evaluation of NBKA toward Expressed UGT2B7-catalyzed AZT glucuronidation. Concentration-dependent plot (a) and Dixon plot (b) of NKBA's inhibition toward recombinant UGT2B7-catalyzed AZT glucuronidation. All experiments were performed in triplicate.

Figure S9 Inhibition evaluation of NBKA toward Expressed UGT2B15-catalyzed 4-MU glucuronidation. Concentration-dependent plot (a) and Dixon plot (b) of NKBA's inhibition toward recombinant UGT2B15-catalyzed 4-MU glucuronidation. All experiments were performed in triplicate.

Figure S10 Inhibition evaluation of NBKA toward Expressed UGT2B17-catalyzed SAHA glucuronidation. Concentration-dependent plot (a) and Dixon plot (b) of NKBA's inhibition toward recombinant UGT2B17-catalyzed SAHA glucuronidation. All experiments were performed in triplicate.

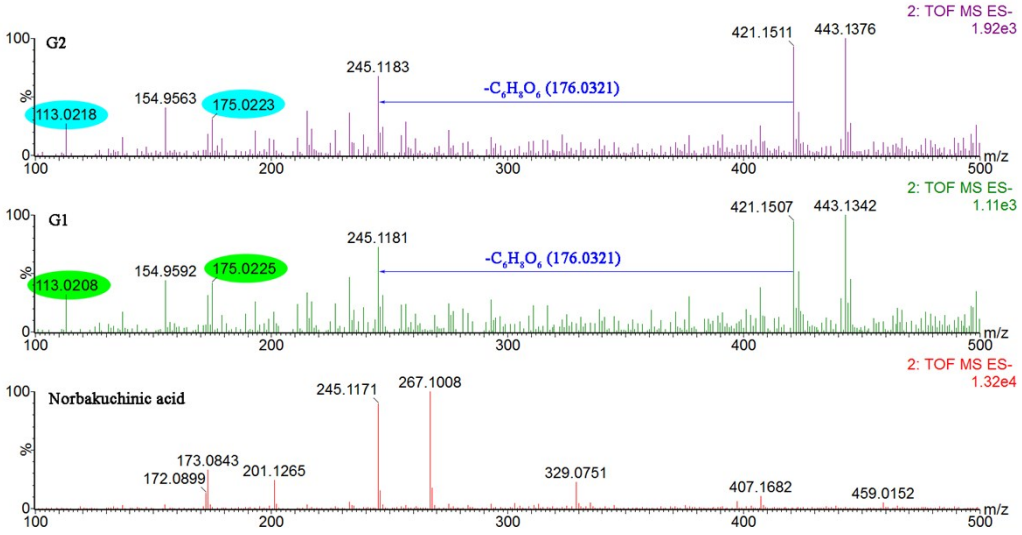

Figure S1 MS/MS spectra of norbakuchinic acid and its two glucuronides.

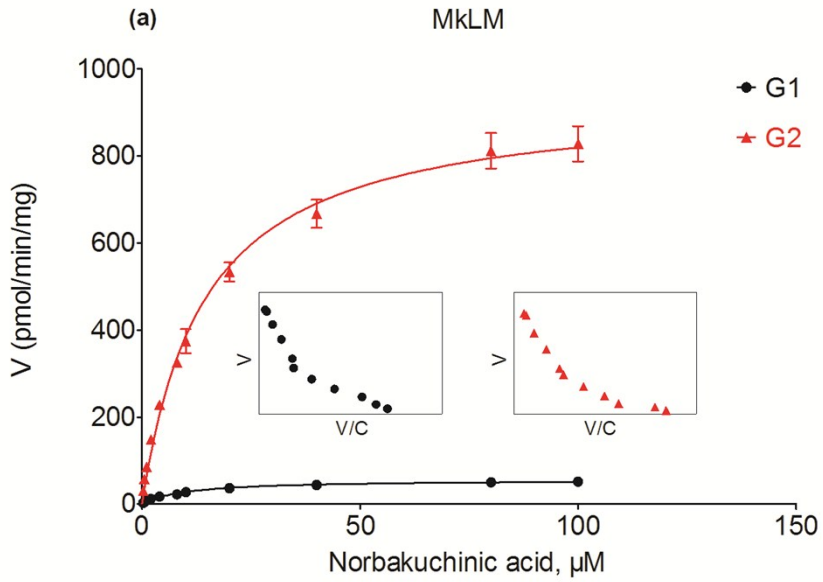

Figure S2-a

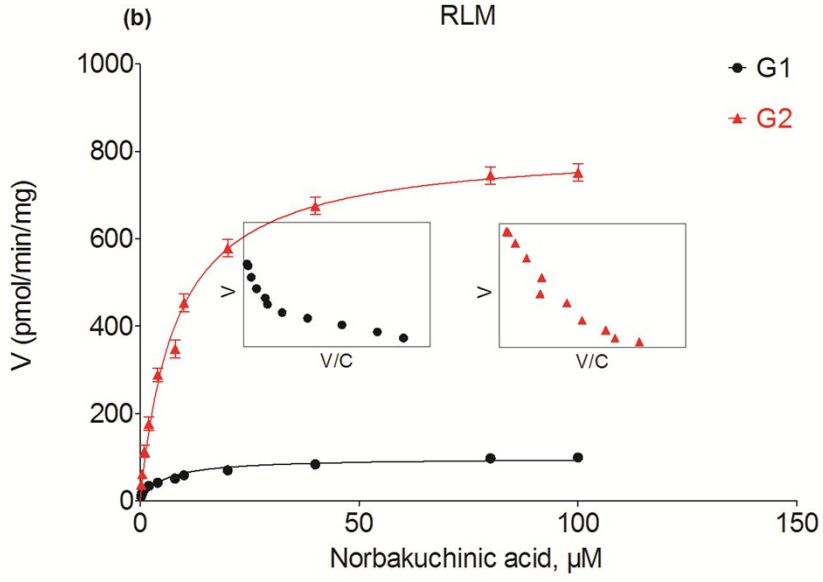

Figure S2-b

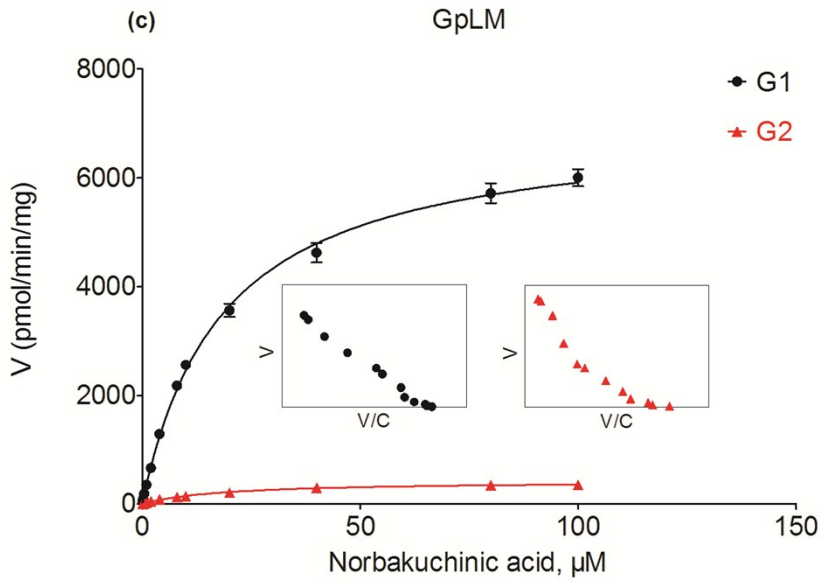

Figure S2-c

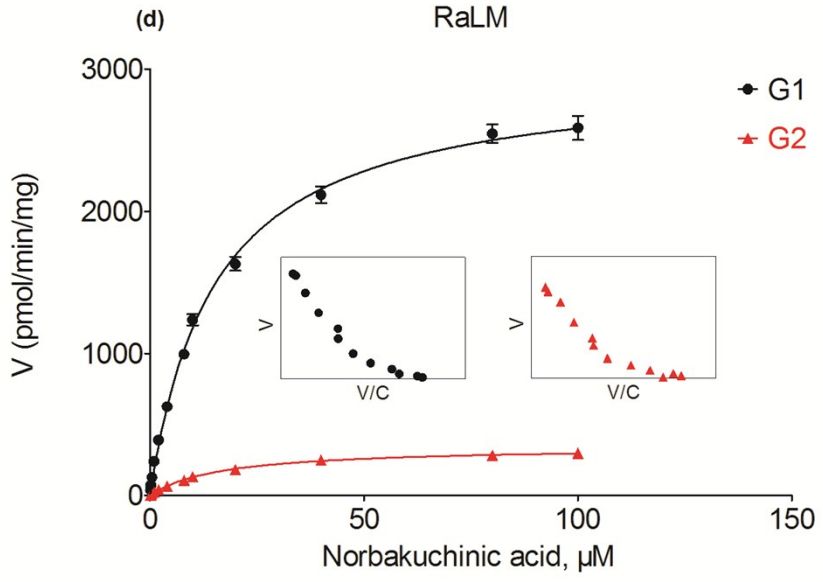

Figure S2-d

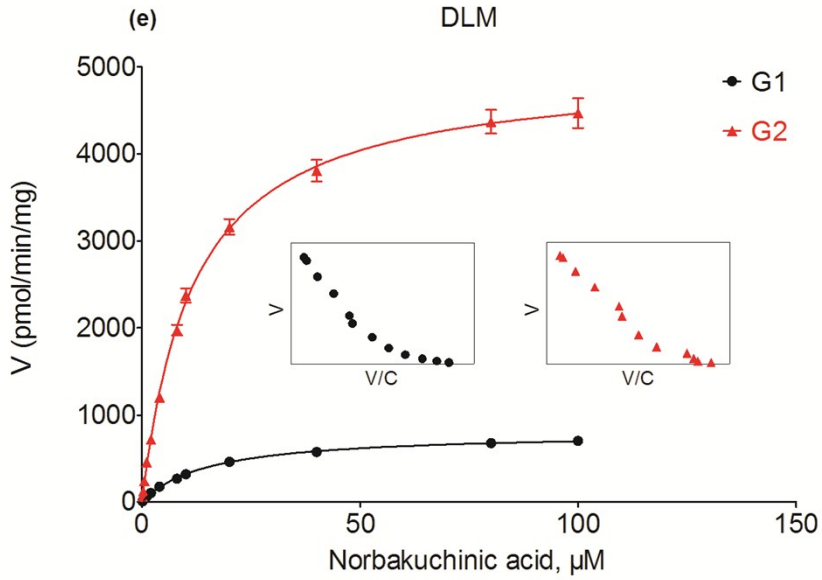

Figure S2-e

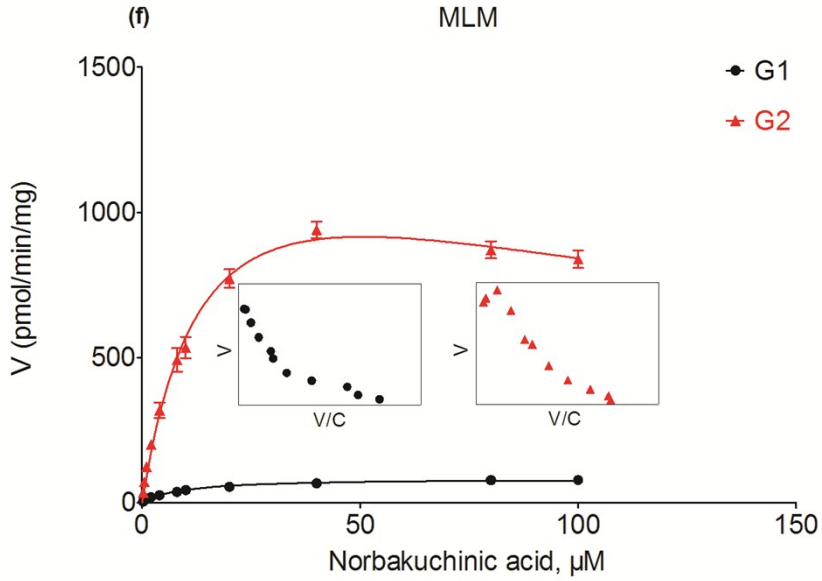

Figure S2-f

Figure S2 Kinectic profiles for glucuronidation of norbakuchinic acid by various types of microsomes. (a) monkey liver microsomes (MkLM); (b) rat liver microsomes (RLM); (c) guinea pig liver microsomes (GpLM); (d) rabbit liver microsomes (RaLM); (e) dog liver microsomes (DLM); (f) mice liver microsomes (MLM); In each panel, the insert figure showed the corresponding Eadie-Hofstee plot. All experiments were performed in triplicate.

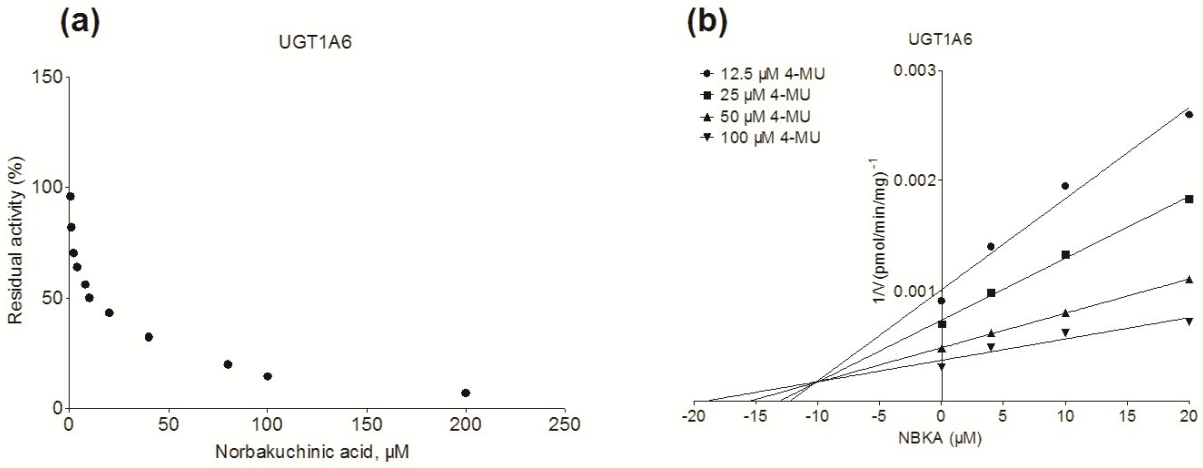

Figure S3 Inhibition evaluation of NBKA toward Expressed UGT1A6-catalyzed 4-MU glucuronidation. Concentration-dependent plot (a) and Dixon plot (b) of NKBA's inhibition toward recombinant UGT1A6-catalyzed 4-MU glucuronidation. All experiments were performed in triplicate.

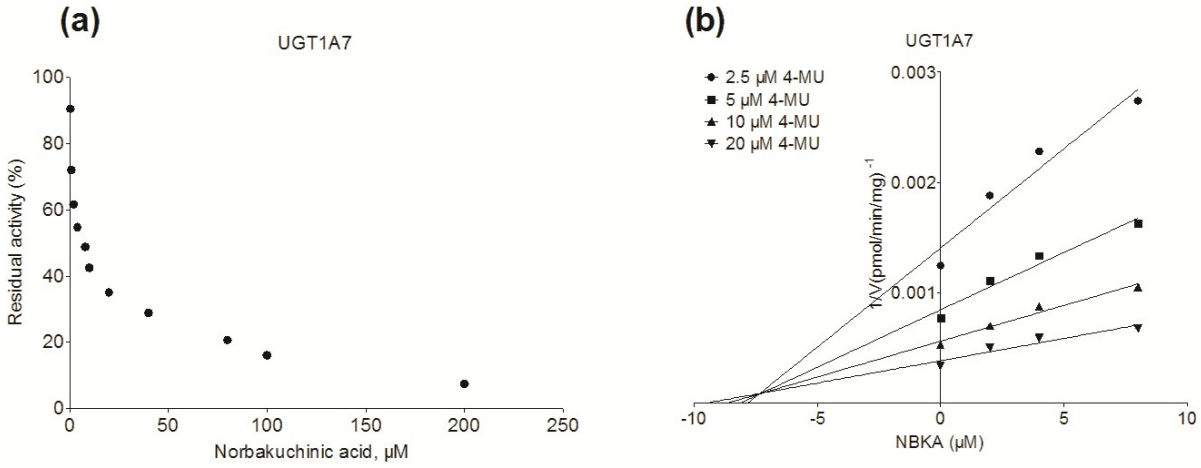

Figure S4 Inhibition evaluation of NBKA toward Expressed UGT1A7-catalyzed 4-MU glucuronidation. Concentration-dependent plot (a) and Dixon plot (b) of NKBA's inhibition toward recombinant UGT1A7-catalyzed 4-MU glucuronidation. All experiments were performed in triplicate.

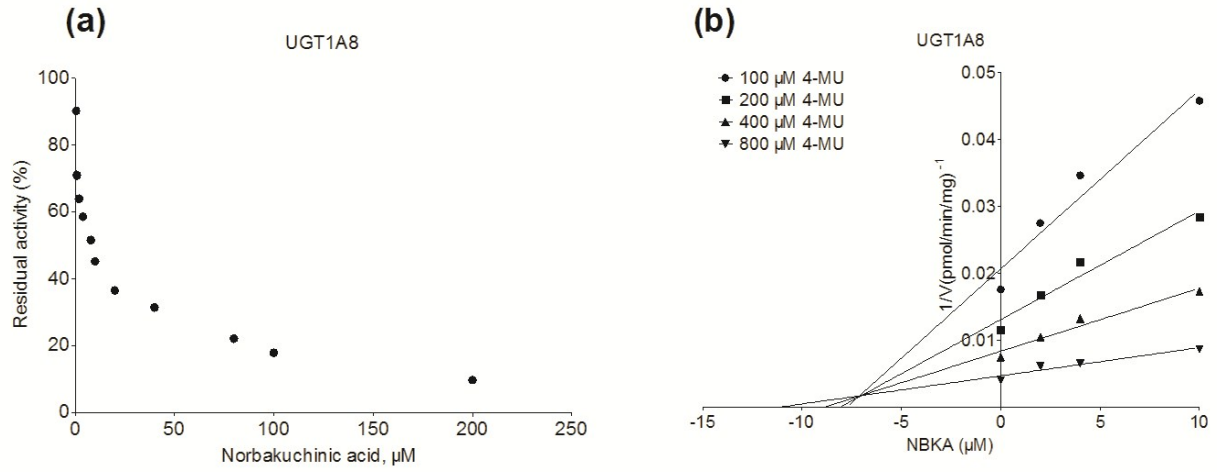

Figure S5 Inhibition evaluation of NBKA toward Expressed UGT1A8-catalyzed 4-MU glucuronidation. Concentration-dependent plot (a) and Dixon plot (b) of NKBA's inhibition toward recombinant UGT1A8-catalyzed 4-MU glucuronidation. All experiments were performed in triplicate.

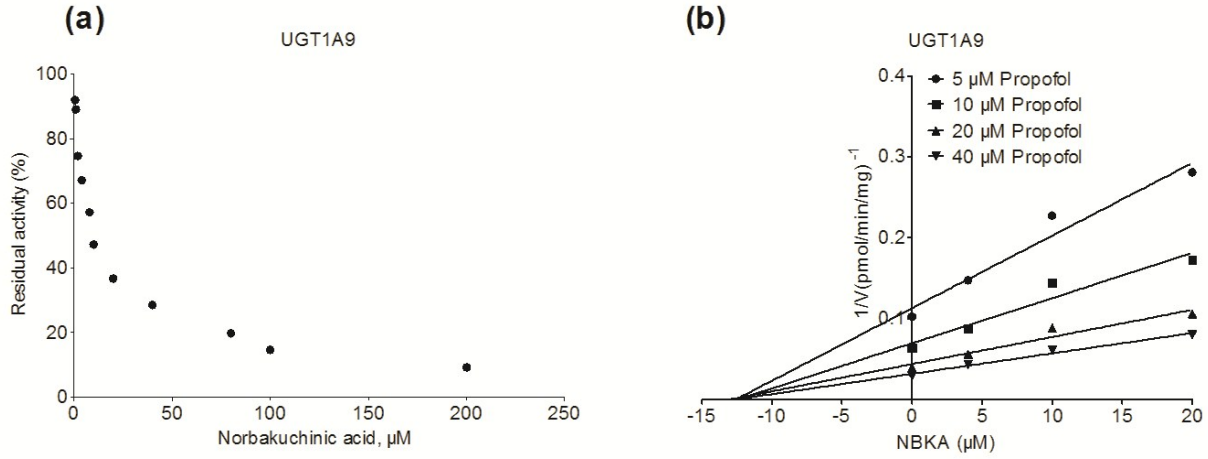

Figure S6 Inhibition evaluation of NBKA toward Expressed UGT1A9-catalyzed propofol glucuronidation. Concentration-dependent plot (a) and Dixon plot (b) of NKBA's inhibition toward recombinant UGT1A9-catalyzed propofol glucuronidation. All experiments were performed in triplicate.

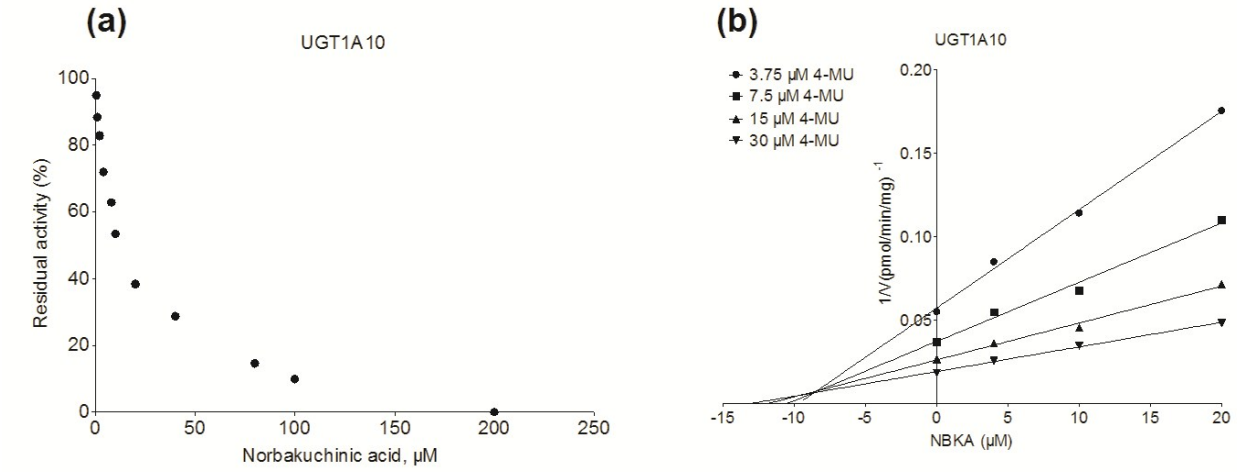

Figure S7 Inhibition evaluation of NBKA toward Expressed UGT1A10-catalyzed 4-MU glucuronidation. Concentration-dependent plot (a) and Dixon plot (b) of NKBA's inhibition toward recombinant UGT1A10-catalyzed 4-MU glucuronidation. All experiments were performed in triplicate.

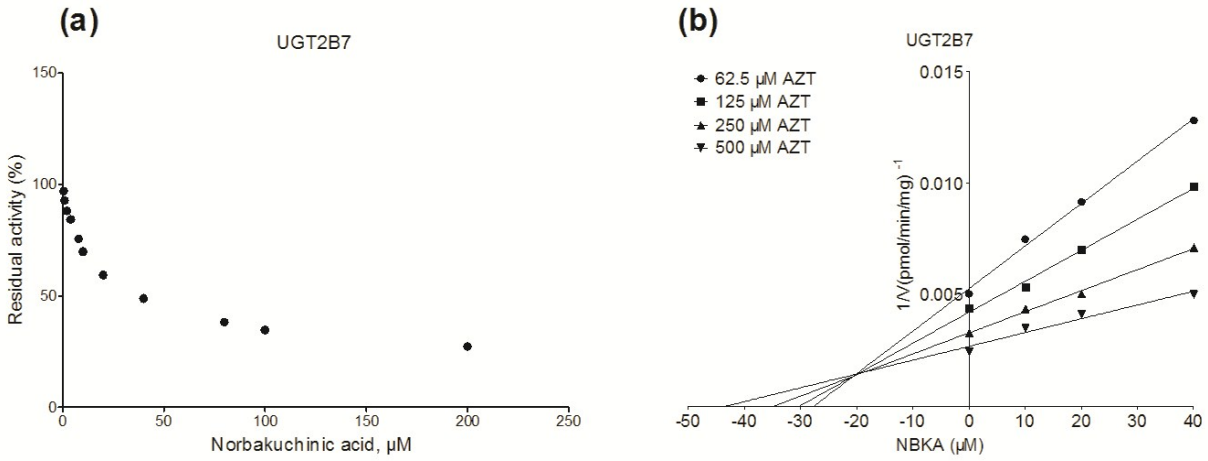

Figure S8 Inhibition evaluation of NBKA toward Expressed UGT2B7-catalyzed AZT glucuronidation. Concentration-dependent plot (a) and Dixon plot (b) of NKBA's inhibition toward recombinant UGT2B7-catalyzed AZT glucuronidation. All experiments were performed in triplicate.

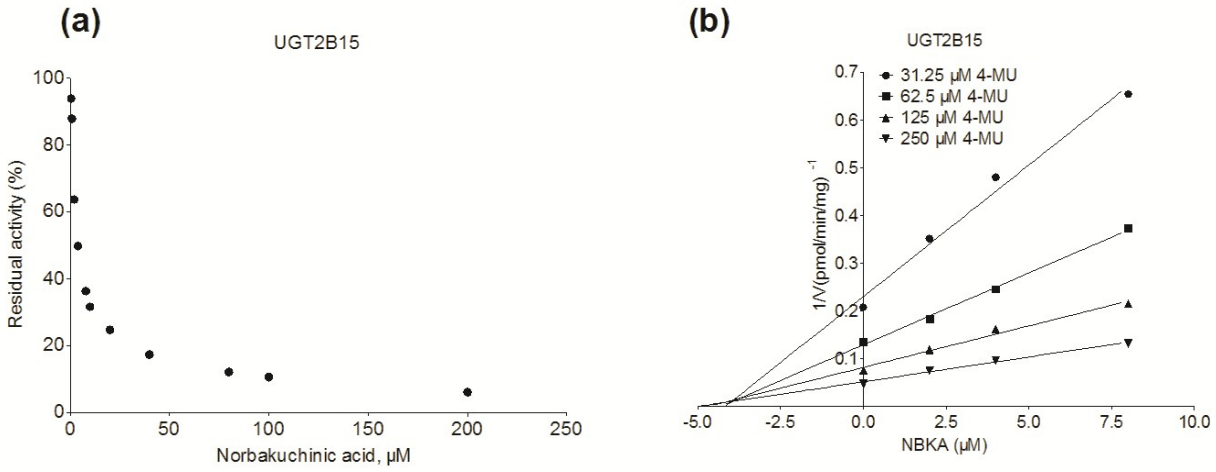

Figure S9 Inhibition evaluation of NBKA toward Expressed UGT2B15-catalyzed 4-MU glucuronidation. Concentration-dependent plot (a) and Dixon plot (b) of NKBA's inhibition toward recombinant UGT2B15-catalyzed 4-MU glucuronidation. All experiments were performed in triplicate.

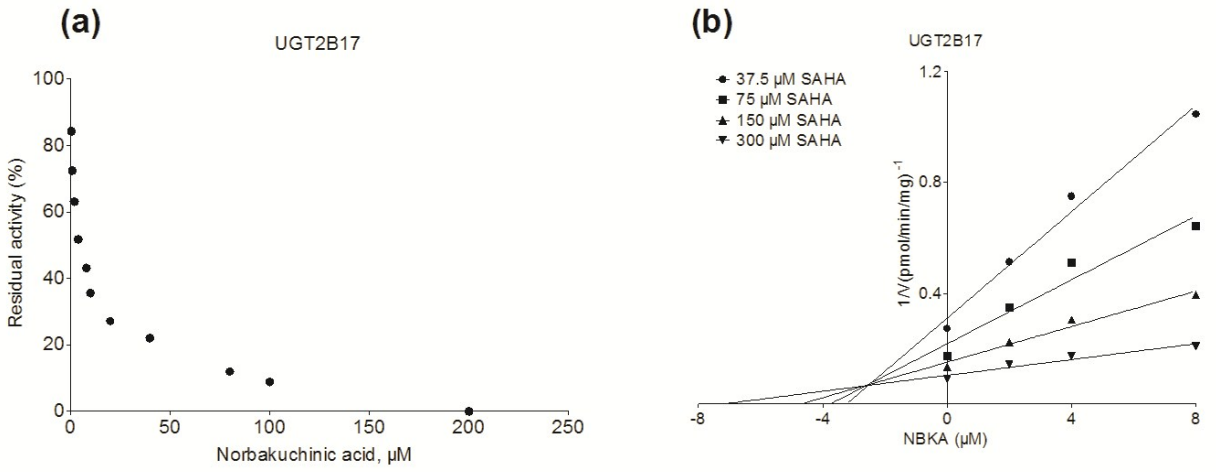

Figure S10 Inhibition evaluation of NBKA toward Expressed UGT2B17-catalyzed SAHA glucuronidation. Concentration-dependent plot (a) and Dixon plot (b) of NKBA's inhibition toward recombinant UGT2B17-catalyzed SAHA glucuronidation. All experiments were performed in triplicate.